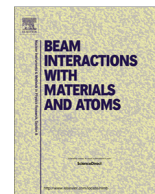




Contents lists available at ScienceDirect

Nuclear Instruments and Methods in Physics Research B

journal homepage: www.elsevier.com/locate/nimb

Kinetics of solid-state reactions between zirconium thin film and silicon carbide at elevated temperatures

E.G. Njoroge^{a,*}, C.C. Theron^a, J.B. Malherbe^a, O.M. Ndwandwe^b^a Department of Physics, University of Pretoria, Pretoria 0002, South Africa^b Department of Physics, University of Zululand, KwaDlangezwa 3886, South Africa

ARTICLE INFO

Article history:

Available online xxxxx

Keywords:

Zr
SiC
Interface
Reactions
Kinetics

ABSTRACT

Solid state reactions between a thin film (133 nm) of Zr and bulk single crystalline 6H-SiC substrates have been studied at temperatures between 600 °C and 850 °C for durations of 30, 60 and 120 min under high vacuum conditions. The deposited film and reaction zones were investigated by Rutherford backscattering spectrometry (RBS) and X-ray diffraction. The RBS spectra were simulated in order to obtain the deposited layer thickness, reaction zone compositions and reaction zone thickness. The as-deposited spectra fit well with those annealed at 600 °C, thus showing there were no reactions taking place. At temperatures of 700 °C and above, Zr reacted with the SiC substrate and formed a mixed layer of Zr carbide (ZrC_x) and Zr silicides (ZrSi, Zr₂Si and Zr₅Si₃). Annealing at 850 °C for 240 min revealed that all the deposited Zr had completely reacted. The interface reaction follows the parabolic growth law thereby indicating diffusion controlled reaction kinetics. The activation energy for the diffusion process obtained was 1.6 eV in the relatively narrow temperature range 700–850 °C.

© 2014 Elsevier B.V. All rights reserved.

1. Introduction

Silicon carbide (SiC) is a ceramic material used in high temperature, high frequency and high power structural and electronic devices [1,2]; conventional semiconductors cannot adequately perform in these conditions. But SiC possesses many favourable chemical, physical and electronic properties for these applications such as; high thermal conductivity, high thermal stability, chemical inertness, high breakdown electric field strength, and wide band-gap [1,2]. SiC in a monolithic ceramic form, is used for fuel kernel encapsulation in tri structural-isotropic (TRISO) particles [3–5]. TRISO fuel particles were developed for use in high temperature gas cooled reactors (HTGRs) like the pebble bed modular reactor (PBMR). SiC is known to provide structural integrity to the fuel kernel and is the main diffusion barrier of metallic fission products in coated fuel particles [3–5].

Zirconium is a transition metal with a high melting point (1850 °C). It has been proposed for use in metal matrix microencapsulated (M3) fuels being developed for use in light water reactors (LWRs) [6,7]. The M3 fuel rod, consist of coated fuel particles embedded in a Zr metal matrix. The Zr yield in most nuclear fuels has been found to be high compared to other fission products [8].

Zr has also been proposed as a stable metal contact to SiC for high temperature electronic operations [9].

The fabrication of M3 fuel rods involves Hot Isostatic Pressing (HIP) and extrusion processes which require high temperatures. These high operating and fabrication temperatures could induce reactions at the Zr/SiC interface of M3 fuels. Reactions between fission products and SiC in TRISO fuel particles are known to decrease the thickness of the SiC layer and may result in fission product release [10]. When SiC based electronic devices are operated at high temperatures and for long durations, degradation or alteration of the device performance is usually observed. The degradation arises from interdiffusion and reactions occurring at the metal/SiC interface [11]. For these applications of SiC as a structural and electronic material, the metal/SiC interactions and their thermal stability are of fundamental importance and need to be understood clearly.

Reactive phase formation in thin films is known to differ from bulk diffusion couples [12], for example, the stable phases formed in thin films are known to form sequentially and metastable compounds can appear in the reaction zone. Previous studies on the Zr/SiC interface have involved the use of bulk Zr metal in contact with SiC [13,14]. In this study, the solid-state reactions between *thin* Zr films and single-crystalline 6H-SiC polytype substrates at elevated temperatures were investigated. The reaction products formed and reaction kinetics are discussed in the temperature range of 600–1000 °C.

* Corresponding author. Tel.: +27 12 420 4777; fax: +27 12 362 5288.

E-mail address: eric.njoroge@up.ac.za (E.G. Njoroge).

2. Experimental method

The 6H-SiC single-crystal wafers were purchased from Pam-Xiamen (China). The bulk semi-insulating wafers, were single-face polished with Si face epiready, 2 inch diameter, 330 μm thick, micro pipe density of $<30\text{ cm}^{-2}$ and with root mean square (rms) surface roughness of less than 0.5 nm. The Zr sputtering target (AJA international Inc.) was 2 inches in diameter and 0.25 inches thick with 99.5% purity. Thin Zr films were sputter deposited on the 6H-SiC wafers by an AJA international Inc. Orion 5 sputtering system. The SiC wafer was mounted on a rotating sample holder to ensure an uniform deposited layer. The chamber was pumped down to a base pressure of 10^{-7} Torr and then backfilled with Ar gas to a pressure of 10^{-3} Torr. The Ar gas flow was kept constant at 8 sscm/min. The Zr target (DC sputtering) and the SiC (RF sputtering) substrate were sputter-cleaned for 10 min using Ar plasma before the room temperature sputtering was done. This ensured the removal of the native oxide layer from the SiC wafer and a clean Zr target surface for sputtering, since Zr readily oxidizes in air.

The sputtering rate of the Zr thin film was calculated to be $\sim 7\text{ nm/min}$ and the sputter time was chosen to achieve a nominal thickness of 140 nm. The Zr/SiC diffusion couples were cleaved into $5 \times 5\text{ mm}$ pieces using a diamond scribe and were placed in a desiccator when not being analysed. The samples were annealed in a (high vacuum) HV quartz tube furnace at temperatures of 600 $^{\circ}\text{C}$, 700 $^{\circ}\text{C}$, 760 $^{\circ}\text{C}$, 800 $^{\circ}\text{C}$ and 850 $^{\circ}\text{C}$ for 30, 60 and 120 min. The furnace was preheated to the desired temperature and then drawn over the quartz tube with the sample inside. After the annealing

time was achieved, the furnace was pulled away from the quartz tube to allow the sample to cool down. This procedure ensured minimum heating and cooling times for the samples. The HV annealing at a base pressure of around 10^{-7} mbar was necessary to reduce oxidation of Zr during the heat treatment. Some of the samples were also annealed at 1000 $^{\circ}\text{C}$ for 120 min to reach the thermal equilibrium state of the Zr/SiC system.

All the samples were analysed by Rutherford backscattering spectrometry (RBS) before and after annealing. The energy of the He^+ ions was 1.6 MeV with a scattering angle of 165° and the sample was tilted by a goniometer to avoid channelling. RBS analysis was performed to obtain the elemental composition of the as-deposited and annealed samples, the thickness of deposited Zr film and the thickness of the reaction zone. Grazing incidence X-ray diffraction (GIXRD) and wide angle XRD analysis done using a Bruker D8 Advanced XRD system with a $\text{CuK}\alpha$ X-ray radiation source. For GIXRD analysis, the X-ray incident beam angle was kept at an angle of 3° relative to the surface of the sample and the diffraction pattern collected by a detector rotated by a goniometer from 15° to 90° . Wide-angle XRD analysis was also performed on the as-deposited and annealed samples. The two-theta radiation source angle was maintained at 20° and the detector angle scan was from 20° to 110° .

3. Results and discussion

The aim of this study was to investigate the phases formed at the Zr/SiC interface and the reaction kinetics of the system.

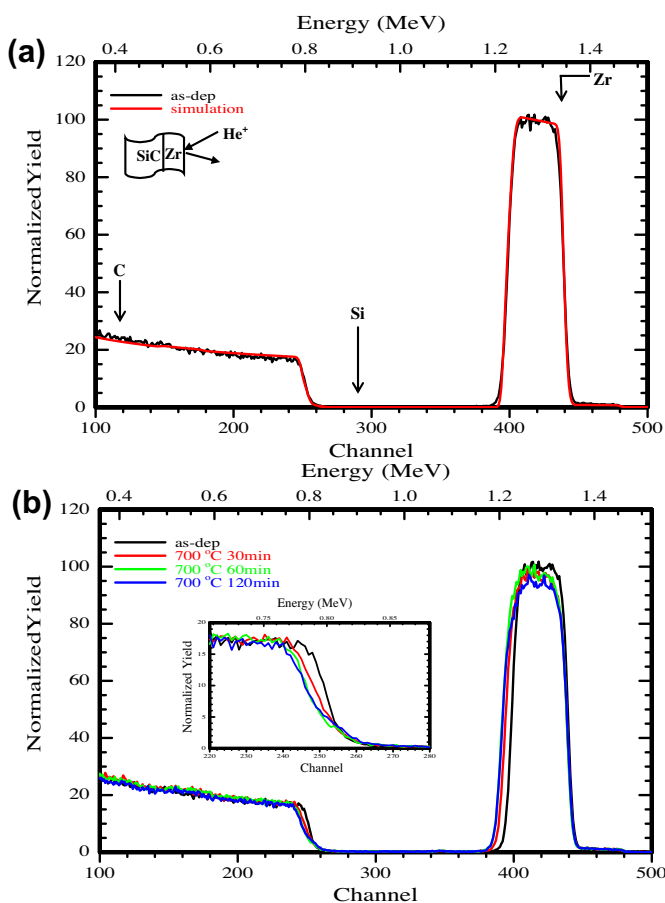


Fig. 1. (a) Raw RBS spectra of as-deposited Zr/SiC with RUMP simulation spectrum. (b) Overlay of as-deposited and 700 $^{\circ}\text{C}$ annealed samples with insert of magnified portion from channel 200–300.

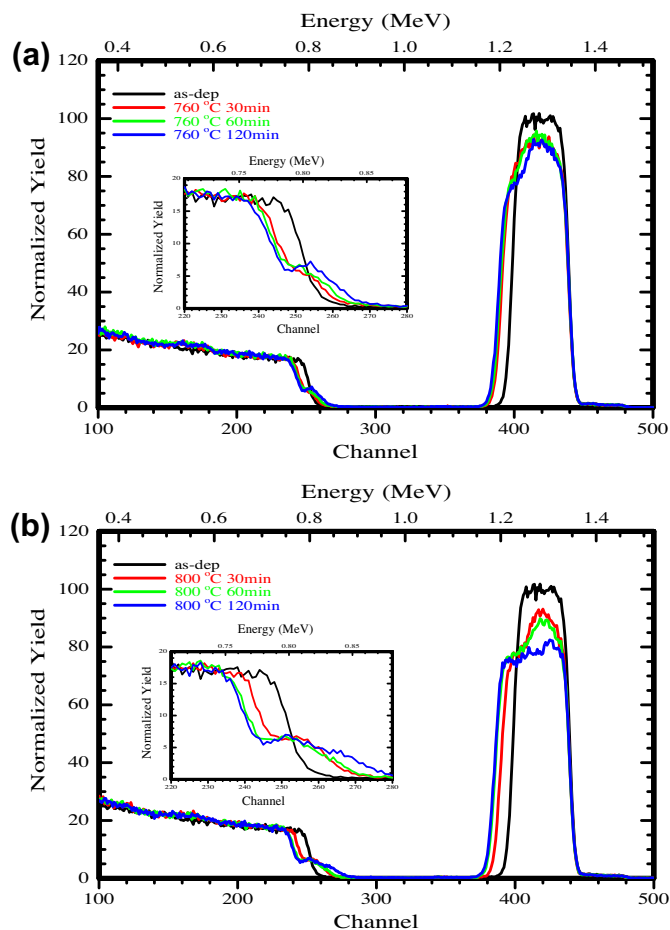


Fig. 2. (a) Overlay of RBS spectra of as-deposited and 760 $^{\circ}\text{C}$ and (b) 800 $^{\circ}\text{C}$ annealed samples with inserts of magnified portion from channel 200–300.

According to the ternary phase diagram of Zr–Si–C system at 1200 °C [15], interface reactions are expected to occur between Zr and SiC since no tie-line exists between the Zr and SiC phases. SiC reacts with most metals and the reaction temperatures of SiC with metals are usually greater than those of Si with the same metals [16]. The reaction products formed at the interface and the interface morphology of metal/SiC reaction zone is dependent on the metal in contact with SiC [17]. For example, refractory metals form carbides and silicide when in contact with SiC since they are strong carbide forming metals [18].

RBS spectra were obtained after each annealing time to determine the growth rate of the Zr/SiC reaction zone. The RBS spectra of the as-deposited Zr/SiC sample is displayed in Fig. 1(a) along with the simulated spectra done using the RUMP [19] computer code. The arrows indicate the surface positions of the respective elements. The as-deposited Zr film exhibits a step starting at 1.42 MeV; this is attributed to hafnium which inherently occurs in Zr metal in trace amounts. From the RUMP simulations, the Hf concentration in the deposited layer is about 0.2%. The thickness of the as-deposited Zr film was calculated using RUMP and was found to be 133 nm. All the spectra of samples annealed at 600 °C were found to perfectly overlay with the as-deposited samples and hence are not reported here.

The RBS spectra of the as-deposited and annealed samples at 700 °C for 30 and 60 min as seen in Fig. 1(b), shows a reduction in the Zr peak height with increasing annealing time. After

annealing, the back edge (lower energy) of the Zr signal has a progressive shift towards lower energy channels. A similar shift is observed on the high energy Si edge, which tends to shift toward lower energy channels with annealing time; this indicates that interdiffusion is taking place. For reactions to occur at the interface, SiC has to dissociate to its elemental constituents, that is, carbon and silicon [16]. This dissociation of SiC can be catalytically enhanced by the reaction metal, because the accepted dissociation temperature of SiC is 2700 °C [3]. However, it must be noted that SEM investigations have shown that the surface decomposition of SiC is already visible at 1300 °C [20]. After dissociation, C and Si then diffuse from the interface into the Zr metal and Zr diffuses from the interface into SiC. Although just visible for 60 min anneal, especially, the sample annealed at 700 °C for 120 min, shows there is a reduction in height and a further shift to lower energies of the Zr signal, this is accompanied with the appearance of a small step at the high energy edge of the Si signal. This is a clear indication of the beginning of formation of Zr silicides.

This shift to higher energies by Si is observed to increase with the annealing duration indicating a growing reaction zone. These results indicate that the Zr/SiC interface begins to react at temperature of 700 °C with the formation of zirconium carbide and silicides. Annealing at 760 °C and 800 °C, the step on the Si edge continues to grow towards the Si surface channel indicating lateral growth of the reaction zone. It can also be observed in Fig. 2(a) and (b) that a step starts to develop on the low energy side of the Zr

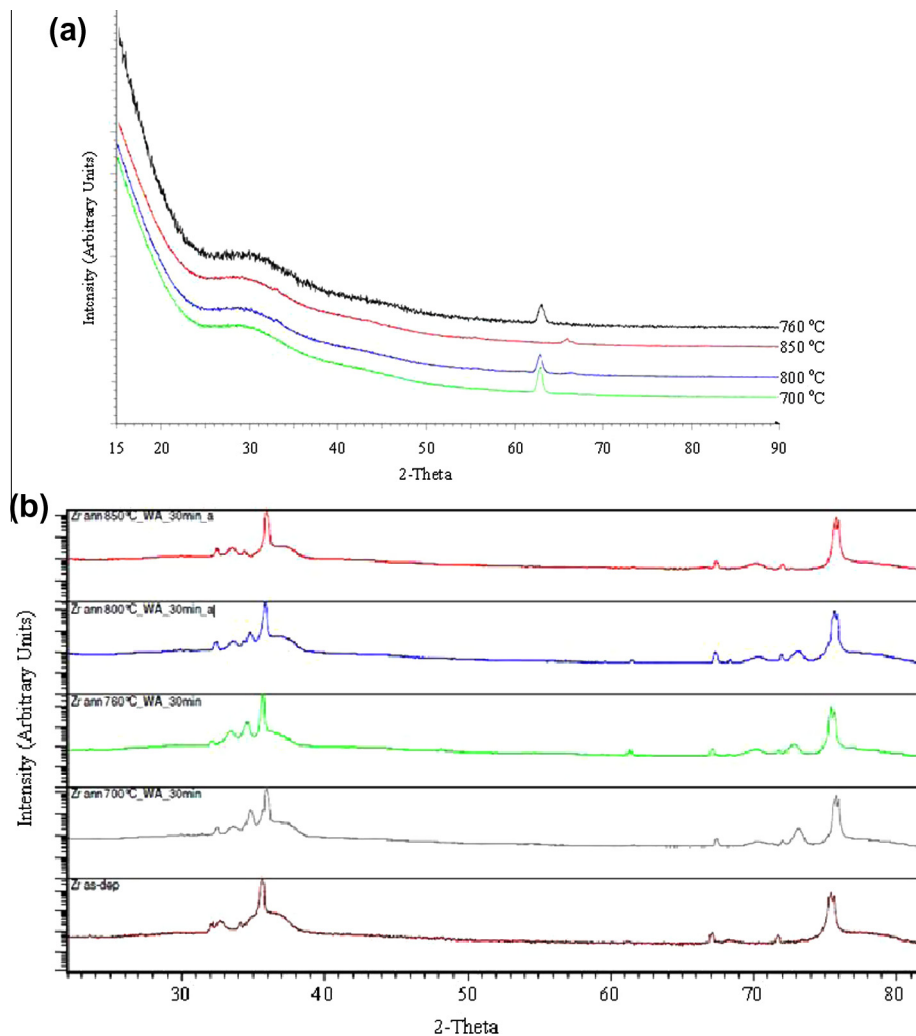


Fig. 3. (a) GIXRD and (b) wide angle XRD spectra of as-deposited, annealed at 700 °C, 760 °C, 800 °C, 850 °C and 900 °C samples.

signal. This step gets wider with increase in annealing temperature up to 850 °C spectra not shown. At this temperature, a plateau appears at the top of the Zr signal, which indicates that the deposited Zr layer has fully reacted with SiC. The Si signal appears at its surface channel position after annealing at 850 °C for 120 min indicating that Si is present from the shifted interface all the way to the surface of this sample. The comparison of the Zr peak total areal counts of the as-deposited with the annealed samples was found to remain constant indicating that there was no loss of deposited Zr atoms due to delamination during the annealing process. The solid-state reactions at the Zr/SiC interface appear to have stopped when the sample was annealed at 850 °C for 120 min. Further annealing at this temperature for four hours and at 900 °C and 1000 °C for two hours, reveals no changes in the reaction zone. The RBS spectra of samples annealed at 900 °C and 1000 °C exactly overlay those of samples annealed at 850 °C for two hours indicating that the reactions have stopped and the system is at a state of equilibrium, these spectra have not been reported here.

XRD measurements were performed to identify the phase and crystallinity of the deposited thin film and phases formed in the reaction zone. Grazing incidence X-ray diffraction spectra of samples annealed from 700 °C to 850 °C for 30 and 60 min (see Fig. 3 (a) and (b)) revealed that the deposited thin Zr film was amorphous. After thermal annealing, some crystalline phases were observed to be forming at the Zr/SiC interface. Wide-angle XRD analysis was performed on the as-deposited and annealed samples since diffraction peaks could not be picked from GIXRD analysis of the samples. The wide angle XRD spectra of as-deposited sample revealed peaks of unreacted Zr and SiC substrate, but no zirconium silicide or carbide peaks were seen. For the sample annealed at 1000 °C for 2 h, no unreacted Zr was visible, but a strong peak from the SiC substrate can be observed. The various Zr silicide and carbide phases Zr_2Si , $ZrSi$, Zr_5Si_3 and ZrC are observed to be present.

From the Zr–Si–C ternary phase diagram [13] there is only one phase in either of the Si–C and Zr–C binary systems, that is, SiC and ZrC respectively. The Zr–Si side of the ternary phase diagram shows that there are seven silicides that can occur and since no tie-line exists between Zr and SiC, these reactions are expected to occur. Zr is a strong carbide former based on the negative enthalpies of formation. ZrC has a value of -202.9 kJ/mol [21] which is much lower than all the silicides occurring in the system and is expected to be the dominant phase in the reaction zone.

A kinetics study was performed by measuring the growth of the total reaction zone thickness as a function of time at different temperatures. Four different temperatures (700 °C, 760 °C, 800 °C, 850 °C) were used in this study and samples were annealed for three different time durations (30, 60, 120 min) at each temperature. In reaction kinetics investigations, it is important to identifying the reaction mechanism, namely, diffusion-controlled or reaction-controlled, the activation energies and corresponding pre-exponential factors. The Zr/SiC interface reaction was assumed to be diffusion-controlled because the growth of the reaction layer followed a parabolic growth law with respect to annealing time. The resulting squares of the interface layer thickness were plotted against the annealing time as seen in Fig. 4(a). Straight lines were obtained using a linear fit at the particular annealing temperatures. The growth of compounds at an interface between dissimilar materials is often expressed as $(x-x_0)^2 = kt$, where x is the distance from original interface x_0 to new interface, t is the annealing duration, and k is the reaction rate constant. This equation gives the parabolic relationship between the thickness of the reaction zone and time. The activation energy for the reaction zone growth is obtained from the Arrhenius-type equation, $k = k_0 \exp(-Q/RT)$, where k is the reaction rate constant for growth, k_0 is the pre-exponential factor, Q the activation energy for the growth of the reaction zone (i.e. the interdiffusion of the reaction species), T the temperature in

Kelvin and R the gas constant [22]. The reaction rate constant k , is dependent on the annealing temperature, as can be observed in Fig. 4(a). The annealed Zr–SiC reaction zone was observed to grow following the parabolic law. This type of growth indicates that the reaction between Zr and SiC was controlled by a diffusion process. From the Arrhenius plot in Fig. 4(b) we obtained the activation energy, Q of 1.6 eV and pre-factor k_0 equal to 3.6×10^{-4} cm²/s. The data can be fitted by a single activation energy in this temperature range. This indicates that one particular diffusing step is rate limiting [23]. The activation energies measured by Thompson and Tu [24] for growth processes of silicides has been found to range between 1.1 and 1.5 eV. These values are low and are indicative of grain boundary diffusion process.

Similar studies on the interface reactions between bulk films of Zr on SiC have been done. The phases formed in the Zr/SiC reaction zone observed by Fukai [13] are similar to those by Bhanumurthy and Schmid-Fetzer [14]. These include: granular ZrC_x , Zr_2Si , ZrC and a ternary phase $Zr_5Si_3C_x$. Bhanumurthy and Schmid-Fetzer also performed a kinetic study of the Zr/SiC system and parabolic growth was observed for the phases formed in the whole reaction zone. They obtained activation energy, Q as 1.4 eV and pre-exponential factor k_0 equal to 3.4×10^3 μm/s^{1/2} (1.2×10^{-1} cm²/s). The activation energy is close to the value obtained in this study. Although the investigations of Bhanumurthy and Schmid-Fetzer involved bulk Zr film on SiC, the fact that the activation energy for the bulk film case is close to the thin film case indicates that grain boundary diffusion dominates in both cases.

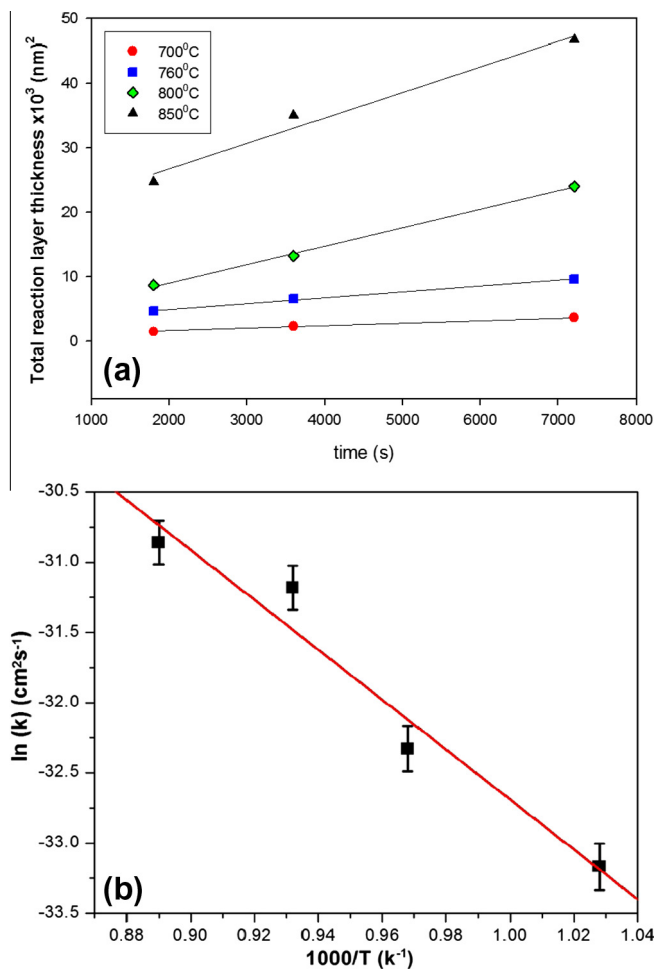


Fig. 4. (a) Plot of the square of the thickness of the reaction zone versus annealing time for the reaction between Zr and SiC at 700–850 °C (b) An Arrhenius plot of the Zr/SiC reaction constant k .

The reactions at the Zr/SiC interface have practical implications. It explains the failure of Zr contacts on SiC for electronic applications at high temperatures and also the degradation of Zr/SiC interfaces in structural composite applications. There is a discrepancy between silver diffusion coefficients in the SiC layer in TRISO particles measured in a reactor and in laboratories [25]. One of the explanations for this discrepancy is the influence of reactions between the SiC and other metallic fission products like Pd, which also forms a silicide [26]. Since Zr is also a fission product, the reactions between Zr and SiC have implications for the integrity of the SiC layer in the TRISO particle.

4. Conclusion

It is observed that the metal Zr reacts with SiC in a relatively narrow range of temperature. The Zr/SiC interface interdiffusion starts at 700 °C. The carbide ZrC and metal rich silicides start forming at the Zr/SiC interface at a temperature of 700 °C and annealing period of 120 min and are present at 760 °C, 800 °C and 850 °C. It is observed that Zr initially diffuses into SiC with the formation of metal rich silicides and ZrC with higher reaction rates measured at high temperatures. Reaction zone and hence the thinning of the SiC substrate is diffusion controlled and grows parabolic with time. The reactions at the Zr/SiC interface could explain the failure of Zr contacts on SiC for electronic applications at high temperatures and the degradation of Zr/SiC interfaces in structural composite applications.

Acknowledgement

The authors wish to thank Mr. T. Ntsoane and Dr. A. Venter from Necsa for their assistance with XRD analysis.

References

- [1] V. B. Shields, "Applications of Silicon Carbide for High Temperature Electronics and Sensors", NASA Jet Propulsion Laboratory, Tech Briefs 0145-319X, 1996.
- [2] P.G. Neudeck, SiC Technology, The VLSI Handbook, The Electrical Engineering Handbook Series, CRC Press Inc., Boca Raton, FL, 2007, pp. 5.1–5.34.
- [3] L.L. Snead, T. Nozawa, Y. Katoh, T.S. Byun, S. Kondo, D.A. Petti, J. Nucl. Mater. 371 (2007) 329–377.
- [4] J.B. Malherbe, E. Friedland, N.G. Van Der Berg, J. Nucl. Instr. Meth. Phys. Res. B266 (2008) 1373–1377.
- [5] E. Friedland, N.G. Van Der Berg, J.B. Malherbe, J.J. Hancke, J. Barry, E. Wendler, W. Wesch, J. Nucl. Mater. 410 (2011) 24–31.
- [6] C.H. Andersson, R. Warren, Composites 15 (1984) 16–24.
- [7] K.A. Terrani, J.O. Kiggans, L.L. Snead, J. Nucl. Mater. 427 (2012) 79–86.
- [8] R. L. Pearson, T. B. Lindemer, "Simulated fission product oxide behaviour in Triso-coated HTGR fuel", Oak Ridge National Laboratory, Report ORNL/TM-6741, 1979.
- [9] C. Kamezawa, M. Hirai, M. Kusaka, M. Iwami, J. Labis, Appl. Surf. Sci. 237 (2004) 607–611.
- [10] R. L. Pearson, R. J. Lauf, T. B. Lindemer, "The Interaction of Palladium, the Rare Earths, and Silver with Silicon Carbide in HTGR Fuel Particles", Oak Ridge National Laboratory, Report ORNL/TM-8059, 1982.
- [11] L. Chen, G.W. Hunter, P.G. Neudeck, D. Knight, J. Vac. Sci. Technol. A16 (5) (1998) 2890–2895.
- [12] R.W. Balluffi, J.M. Blakely, Thin Solid Films 25 (1975) 363–392.
- [13] T. Fukai, M. Naka, J.C. Schuster, Trans. JWRI 25 (1996) 59–62.
- [14] K. Bhanumurthy, R. Schmid-Fetzer, Composites A32 (2001) 569–574.
- [15] Y. Wang, A.H. Carim, J. Am. Ceram. Soc. 78 (1995) 662–666.
- [16] T.C. Chou, A. Joshi, J. Wadsworth, J. Vac. Sci. Technol. A9 (1991) 1525–1534.
- [17] F. Goesmann, R. Schmid-Fetzer, Mater. Sci. Eng. B46 (1997) 357–362.
- [18] J.S. Park, K. Landry, J.H. Perepezko, Mater. Sci. Eng. A259 (1999) 279–286.
- [19] L.R. Doolittle, Nucl. Instr. Meth. B9 (1985) 344–351.
- [20] N.G. Van Der Berg, J.B. Malherbe, A.J. Botha, E. Friedland, Appl. Surf. Sci. 258 (2012) 5561–5566.
- [21] R.C. Weast, Handbook of Chemistry and Physics, 67th ed., CRC Press Inc., Boca Raton, FL, 1986.
- [22] V.I. Dybkov, Reaction Diffusion and Solid State Chemical Kinetics, The IPMS Publications, Kyiv, 2002.
- [23] F. Goesmann, R. Schmid-Fetzer, Semicond. Sci. Technol. 10 (1995) 1652–1658.
- [24] R.D. Thompson, K.N. Tu, Thin Solid Films 93 (1982) 265–274.
- [25] J.B. Malherbe, J. Appl. Phys. 46 (2013) 1–27.
- [26] E.J. Olivier, J.H. Neethling, J. Nucl. Mater. 432 (2013) 252–260.